# A Novel Power-Amplifier Module for Quad-Band Wireless Handset Applications

Shuyun Zhang, *Member, IEEE*, Jelena Madić, *Member, IEEE*, Pavel Bretchko, *Member, IEEE*, Julius Mokoro, Raymond Shumovich, and Rob McMorrow

***Abstract*—This paper presents a novel power-amplifier module (PAM) designed for GSM850-, GSM900 MHz, DCS1800- and PCS1900-MHz handset applications. The module combines an InGaP HBT power-amplifier integrated circuit, two integrated couplers, a dual-band logarithmic RF power detector/controller, and some additional passive components. The logarithmic RF power detector was implemented in the module to accomplish linear-in-decibel output power dependency. This allows the handset manufacturers to calibrate output power ($P\mathrm{out}$) at one or two points, with error as low as $+/-0.3$ dB, thus reducing test time in mass production. Due to higher accuracy, our novel design significantly reduces the power consumption during normal operation. Our design is the first to include two integrated directional couplers in a handset RF PAM. It significantly improves power control accuracy over load variations. In this paper, we show that the directivity of the integrated couplers is critical for establishing accurate power control over phase variations at high values of load mismatch. In addition, the presented module features fully integrated impedance matching at input and output ports with dc blocks. The entire module is plastic encapsulated on a 10 mm $\times$ 10 mm laminate substrate. The module offers higher accuracy of $P\mathrm{out}$ control, smaller size, lower bill-of-materials, and a shorter $P\mathrm{out}$ calibration time to handset manufacturers. It is a very desirable RF PAM to handset designers because of its unique features. Under a low single supply voltage of 3.2 V, the PAM provides 35-dBm output power, 55% power-added efficiency (PAE) in the GSM900 band, and 33 dBm and 50% PAE in the DCS1800 band.**

***Index Terms*—Directional coupler, logarithmic amplifier (log-amp), power amplifier (PA).**

## I. Introduction

As WIRELESS communication systems migrate to third generation (3G), it is desirable to increase the degree of integration of RF front-end integrated circuits (ICs), such as low-noise amplifiers (LNAs), power-amplifier modules (PAMs), surface acoustic-wave (SAW) filters, duplexers, and transmit/receive (T/R) switches. RF design engineers are challenged to provide a system-in-package (SIP) solution to customers. This is particularly true for PAMs. The PAM is a challenging device to many designers because of its many strict system specifications and high degree of integration. The power amplifier (PA) is the most critical device in the front-end. It determines very important system parameters such as talk time, standby time, cost, and size. It is a great deal of work for handset designers to develop a PA and the surrounding circuitry. This makes the drop-in type of PAM a very attractive option.

Manuscript received April 18, 2003; revised June 30, 2003.

The authors are with Analog Devices Inc., Wilmington, MA 01887 USA (e-mail: shuyun.zhang@analog.com).

Digital Object Identifier 10.1109/TMTT.2003.818585

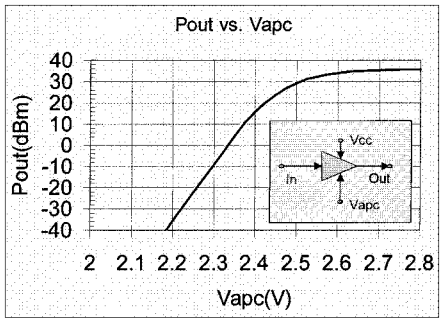


Fig. 1. Typical $P\mathrm{out}$ versus $V apc$.

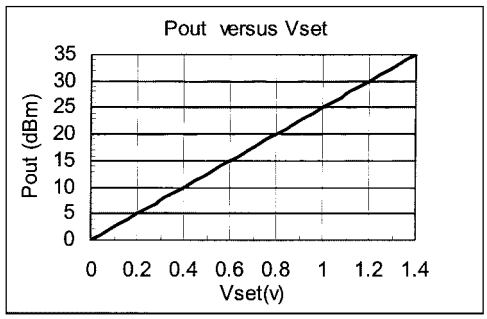


Fig. 2. Linearized $P\mathrm{out}$ versus $V\mathrm{set}$ transformation.

In general, the output power of a PA versus control voltage is not a well-defined function. It takes the handset designers significant time to calibrate and control the output power. Analog Devices Inc., Wilmington, MA, provides a solution to this problem with its logarithmic power detector and PA controller (AD8315 IC) [1]. AD8315's unique features make it useful in managing $P\mathrm{out}$. Our novel PAM has incorporated a modified version of AD8315 IC.

## II. Log-Amp and $P\mathrm{out}$ Control

Usually, a transfer function between the $P\mathrm{out}$ and control voltage $(V apc)$ of a PA is not a linear function [2]. As shown in Fig. 1, the $P\mathrm{out}$ curve is not an easily defined or simple function. This makes it difficult for handset manufacturers to accurately control the output power. Essentially, they have to transform the curve in Fig. 1 into a simpler function such as the linear function shown in Fig. 2, $P\mathrm{out} = a^{*}V\mathrm{set}+b$, where $a$ and $b$ are a slope and an intercept point, respectively. These constants can be determined by a two-point measurement. Once $a$ and $b$ are found, $P\mathrm{out}$ is easily calibrated because it is a linear function of $V\mathrm{set}$. In fact, the accuracy of our controller allows us to ensure that the slope of the curve does not vary significantly from

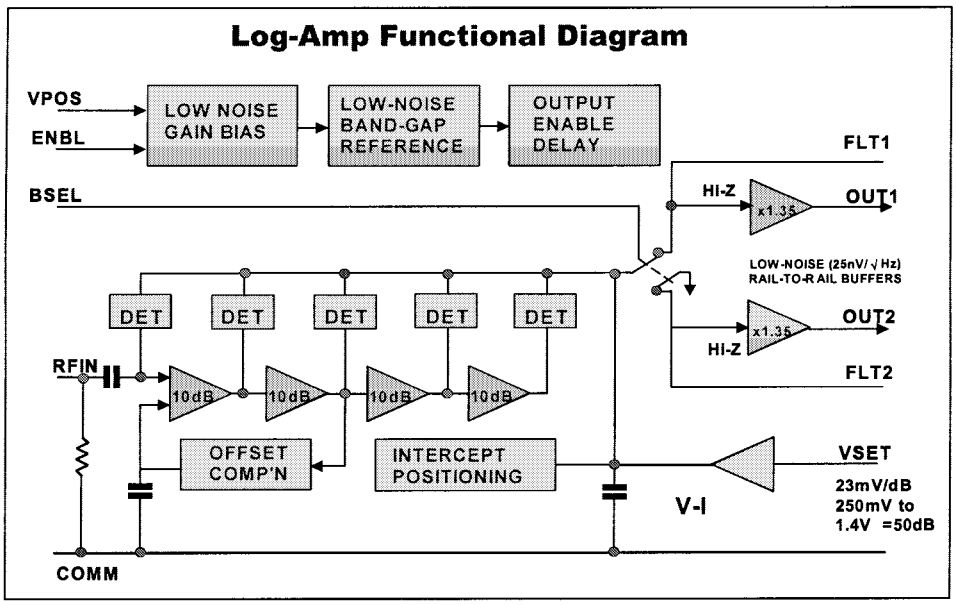


Fig. 3. Log-amp functional diagram.

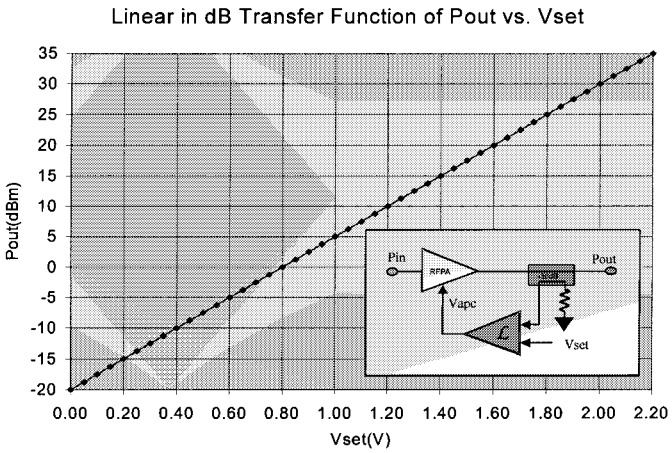


Fig. 4. Demonstration of closed-loop PA with a log-amp power detector and PA controller.

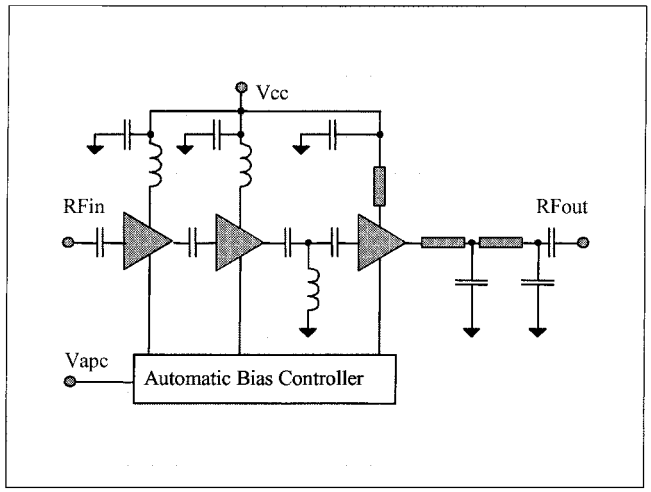


Fig. 5. Block diagram of the presented three-stage PA.

part to part. This enables a single-point calibration to be performed, further reducing associated costs for the original equipment manufacturer (OEM).

A translinear circuit, such as a logarithmic amplifier (log-amp), can implement the above transformation. The AD8315 was designed based on a log-amp. It is a complete sub-system for RF power detecting and controlling. Fig. 3 shows a simplified block diagram of the power detector and PA controller.

The log-amp is used to detect the coupled RF power level and produce an output current $Ip$. The control voltage $V\mathrm{set}$ is transformed into output current $I\mathrm{set}$. $I\mathrm{set}$ is compared with $Ip$ to produce an error current $Ie$. $Ie$ is then transformed into an output voltage $Vapc$. $Vapc$ is used to force $P\mathrm{out}$ to the desired level. Therefore, $P\mathrm{out}$ (in dBm) is always linearly dependant on $V\mathrm{set}$. Fig. 4 demonstrates an ideal closed-loop configuration of a single-band PA that includes an RF PA, a coupler, a log-amp power detector, and a PA controller. The coupling factor of the coupler must be designed to allow for the maximum dynamic range of the detector.

## III. Circuit Design Consideration

### A. PA Design

Our module is primarily designed for the global system for mobile communication (GSM), digital cellular system (DCS), and personal communication services (PCS) worldwide wireless handset market. Output power for the GSM850 and GSM900 bands in a 50-$\Omega$ system is 35 dBm, for the DCS1800, it is 33 dBm, and for the PCS1900, it is 31.5 dBm [3], [4]. Considering the high gain requirement of approximately 30 dB at full output power levels, a three-stage amplifier was designed. The first stage provides linear gain, while the second stage provides enough power to drive the third stage, which works in a deep saturation state. The third-stage transistor is the most important element in a PA circuit. It is directly related to the PA performance. For our application, it is designed to provide high power and high efficiency while operating with a low voltage power supply of 3.2 V. Our three-stage PA schematic is shown in Fig. 5.

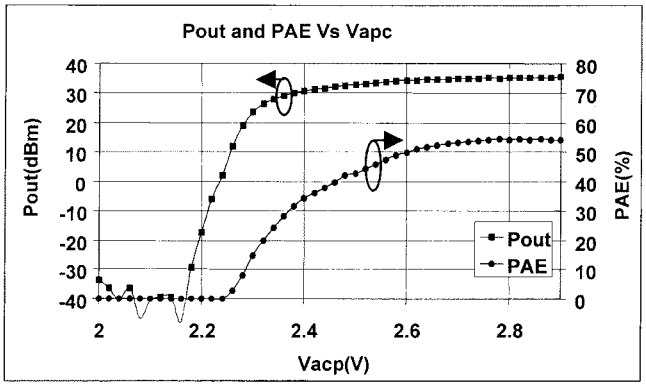


Fig. 6. GSM performance versus control voltage.

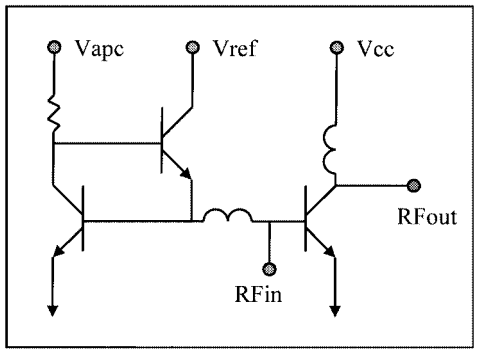


Fig. 7. Current mirror circuit schematic.

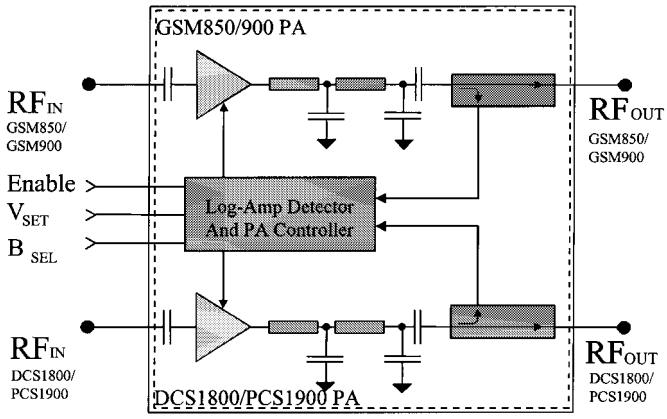


Fig. 8. Simplified schematic of the quad-band PAM.

An InGaP HBT process was used for the PA ICs. The HBT process offered an advantage of operating with a single low-voltage power supply, high power density, and high efficiency. Matching circuits were synthesized with the input and interstage matching circuits realized on-chip. The output matching circuit was implemented outside of the GaAs IC on a module substrate to reduce power loss by taking advantage of high-$Q$ ceramic components. The package parasitics were included in the circuit design from the very beginning and bond-wire inductances were used to help implement the matching networks.

An *RC* feedback loop was also employed on-chip to ensure the stability of the PA. The first stage emitter was connected to ground through a bond wire instead of a via-hole to prevent common mode oscillation. Some resistances were provided at the base of each stage to provide more stability for the PA.

Before incorporating the GSM900 and DCS1800 PAs into the PAM, their individual performances were investigated using evaluation boards. The output matching circuit was implemented using surface-mount components and was adjusted for optimum performance. Typical performance of the GSM900 PA with $Vcc = 3.2$ V versus automatic control voltage $Vapc$ is shown in Fig. 6. It is found that the large-signal gain is 30 dB, $P\text{out} = +35$ dBm with 55% PAE. By sweeping $Vapc$ from 0 to 2.8 V with $\text{Pin} = +5$ dBm, the output power of the GSM900 PA changes from $-40$ to $+35$ dBm. The dynamic range for power control was over 75 dB.

### *B. Bias Circuit*

Much effort was made to design an efficient bias circuit for the PAM. Both amplifiers employ current mirror biasing schemes in order to provide thermal stability of the amplifiers. $Vapc$, provided by the AD8315, sets the gain of the amplifier. Due to the current capability of the customized AD8315, $Vapc$ currents were limited to less then 10 mA, while PAs were driven to saturation. The current mirror circuit schematic is shown in Fig. 7. This bias circuit provides temperature compensation for the bias current $Iapc$.

### *C. Quad-Band Module Design*

As seen in Fig. 6, the function of $P\text{out}$ versus $Vapc$ has quite a steep turn-on region where the output power reaches its maximum with a relatively small change in $Vapc$. It is customary to include external power control circuitry in the handset to linearize the dependence of the PA output power to the control voltage $Vapc$. This results in increased complexity and cost of system design. Our goal was to include the power management circuitry in the PAM to provide a SIP solution to handset designers. Using our AD8315, we have realized this goal.

The top-level block diagram of the complete PAM is illustrated in Fig. 8. The outputs from the GSM900 and DCS1800 PAs are fed into the off-chip output-matching network. The signal is then coupled into the input of the logarithmic power detector of a customized AD8315. The power control circuitry of AD8315 sets the appropriate $Vapc$ to obtain the output power $P\text{out}$. By design, we can adjust the coupling coefficient such that the $V\text{set}$ voltage range is from 0 V, corresponding to the PA being shut off, to 2 V for maximum output power. Therefore, $V\text{set}$ will control the output power of the PAM linearly.

The module was designed for quad-band wireless applications that include GSM850, GSM900, DCS1800, and PCS1900 frequency bands. The band select voltage $B\text{set}$ controlled by a logic level signal is used to select the active operating frequency band of the PAM. The entire PAM can be enabled or disabled by the $\text{Enbl}$ pin.

The output power performance of the multichip PAM was measured as a function of the control voltage $V\text{set}$ for GSM and DCS/PCS bands. The corresponding curves are plotted in Figs. 9 and 10, respectively. Both measurements were performed with the input power level set to $+5$ dBm and a power supply voltage of 3.2 V. Comparing the graphs in Figs. 6 and 9, it is obvious that the closed-loop system exhibits very linear behavior. Therefore, our multichip PAM does not need any extra

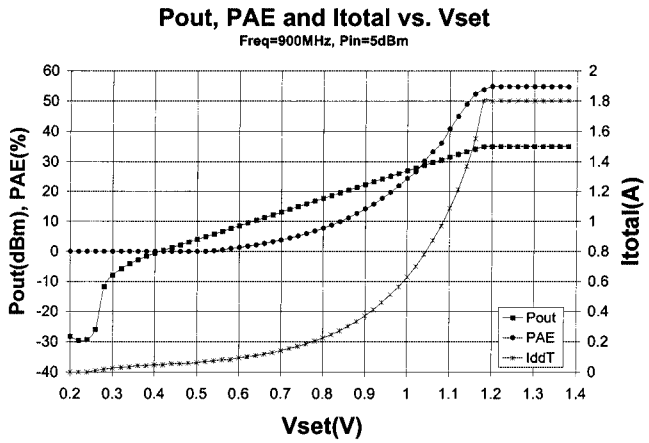


Fig. 9. Output power of the PAM in the GSM band as function of the control voltage $V\mathrm{set}$.

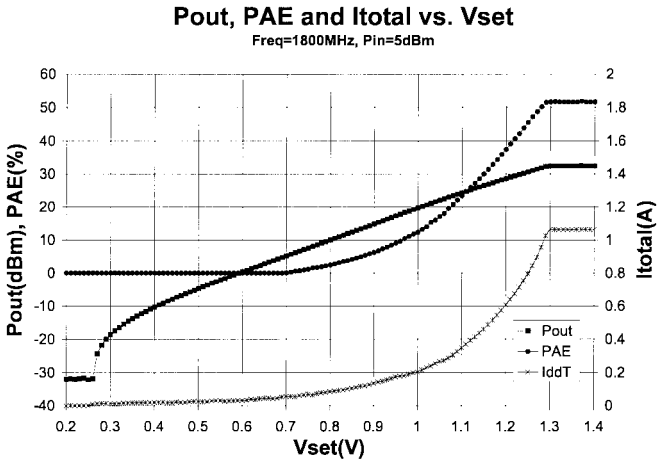


Fig. 10. Output power of the PAM in the DCS band as function of the control voltage $V\mathrm{set}$.

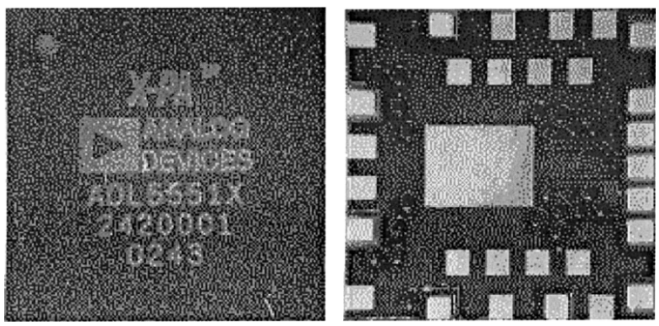

Fig. 11. Top and bottom view of the quad-band PAM.

circuitry for power management. The active $V\mathrm{set}$ range is from approximately 0.3 to 2 V and the linear output power dynamic range for both bands is approximately 50 dB. Fig. 11 shows the PAM. The size of the PAM is 10 mm × 10 mm × 1.5 mm. The PAM features a single low-voltage power supply, high efficiency, and linear-in-decibel output power level control versus $V\mathrm{set}$. Needless to say, this PAM is desirable for handset designers. It eliminates the need for a power management circuitry, therefore, reducing overall size, system complexity, development time, and cost.

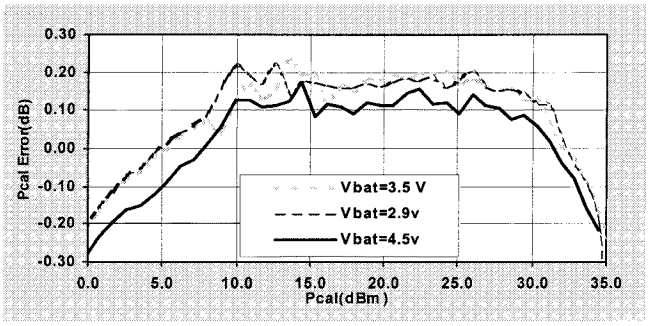


Fig. 12. $P_{\mathrm{cal}}$ error versus $\mathrm{P_{cal}}$ of the PAM in the GSM band at $\mathrm{Pin} = +5$ dBm.

## IV. Assessment of Power Control Accuracy

To assess the linearity of the output power level versus $V\mathrm{set}$, we plotted an error function defined as a deviation of the real output power from the ideal straight line. Such a graph for GSM900 is shown in Fig. 12. The calculated power $(P_{\mathrm{cal}})$ was obtained by calibrating the output power at 5 and 32 dBm, then solving the $P\mathrm{out} = a^{*}V\mathrm{set} + b$ equation to obtain slope $a$ and intercept point $b$. A slope of the calculated power is equal to 46 dBm/V and a corresponding intercept point is −19.1 dBm. Thus, the calculated power $P_{\mathrm{cal}}$ expressed in dBm is

$$P_{\mathrm{cal}} = 46 \cdot V_{\mathrm{set}} - 19.1 \text{ dBm}. \tag{1}$$

The error is then calculated by taking the difference between the actual output power $P\mathrm{out}$ and calculated power $P_{\mathrm{cal}}$ as follows:

$$\mathrm{Error} = P_{\mathrm{out}} - P_{\mathrm{cal}} \text{ dB}. \tag{2}$$

As shown in Figs. 9 and 12, the closed-loop system maintains linearity error of $+/-0.3$ dBm throughout the entire power range and the battery voltage range of the GSM system. The high accuracy of output power control provides significant benefits to customers. First off, it reduces $P\mathrm{out}$ calibration time to one or two measurements while other power control methods typically need more than four measurements. Secondly, high $P\mathrm{out}$ accuracy allows the customer to control $P\mathrm{out}$ close to the lowest transmit power level, which, in turn, saves battery life.

## V. Effect of Integrated Coupler Directivity

A simplified block diagram of the PAM with its internal closed-loop power control circuitry including a directional coupler is presented in Fig. 13.

In Fig. 13, power generated by the PA is fed into the directional coupler. Power delivered to the load $P_{\mathrm{out}}$ is equal to the difference between incident power and power reflected from the load. Under nominal conditions, i.e., when load impedance is equal to 50 Ω, reflected power is equal to zero and power delivered to the load is equal to the power available from the PA, which we denote as $P_{\mathrm{AVS}}$.

For any given load reflection coefficient, the voltage detected at the coupled arm $V_c$ is a vector sum of voltage coupled from the

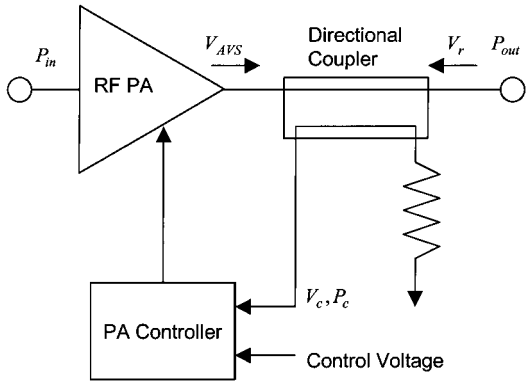


Fig. 13. PAM with integrated directional coupler and power control.

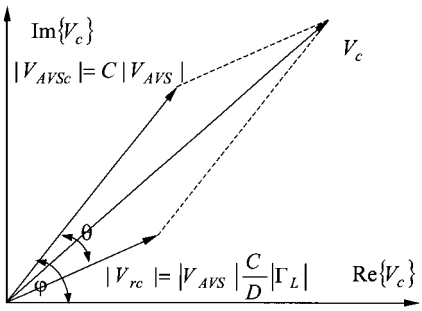


Fig. 14. Magnitude of $V_c$ varies as a function of $\theta$.

forward signal generated by the PA $V_{\mathrm{AVSc}}$ and voltage coupled from the reverse signal reflected by the load $V_{rc}$ as follows:

$$V_c = V_{\mathrm{AVSc}} + V_{rc} = |V_{\mathrm{AVS}}|\left(C + \frac{C}{D}|\Gamma_L|e^{-j\theta}\right) \quad (3)$$

where $C$ is the numerical voltage coupling factor, $D$ is the numerical directivity of the coupler, $|\Gamma_L|$ is the load reflection-coefficient magnitude, and $\theta$ is the phase associated with the load reflection coefficient or the phase difference between the $V_{\mathrm{AVSc}}$ and $V_{rc}$ vectors [5]. We can see from (3) that the magnitude of the $V_c$ vector varies as a function of phase associated with the load. This is illustrated in Fig. 14.

Assuming that the input of the controller is matched to 50 Ω, the power detected at the coupled arm is derived from (3) and is given by

$$P_c = P_{\mathrm{AVS}}\left|C + \frac{C}{D}|\Gamma_L|e^{-j\theta}\right|^2. \quad (4)$$

For any given load, the power controller compares power given in (4) to some set value and adjusts $P_{\mathrm{AVS}}$ in such a way that coupled power is equal to that set value. This will make available power, as well as delivered power, functions of phase. The power delivered to the load in this case is expressed as

$$P_{\mathrm{out}} = P_{\mathrm{AVS}}\left(1 - |\Gamma_L|^2\right). \quad (5)$$

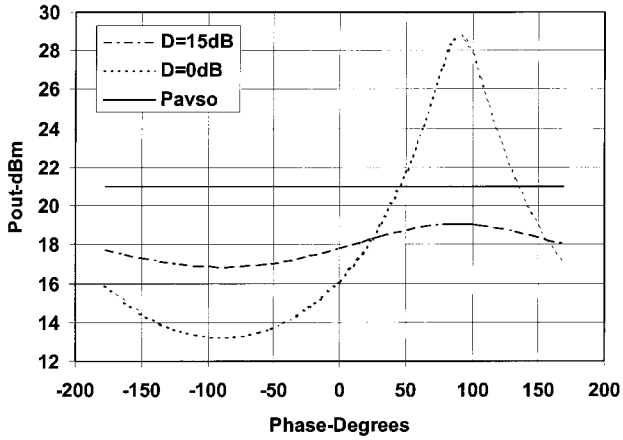


Fig. 15. Delivered power over phase when directivity is 15 and 0 dB, as predicted by (8).

Combining (4) and (5), we get

$$P_{\mathrm{out}} = P_{c0}\cdot\frac{1}{\left|C + \frac{C}{D}|\Gamma_L|e^{-j\theta}\right|^2}\cdot\left(1 - |\Gamma_L|^2\right) \quad (6)$$

where $P_{c0}$ is coupled power for the nominal case when $|\Gamma_L| = 0$ or when the PA is presented with the matched load

$$P_{c0} = C^2 P_{\mathrm{AVS0}}. \quad (7)$$

$P_{\mathrm{AVS0}}$ is the available power in watts when the PA is presented with the matched load. Finally, we can express delivered power as

$$P_{\mathrm{out}} = P_{\mathrm{AVS0}}\cdot\frac{1}{\left|1 + \frac{1}{D}|\Gamma_L|e^{-j\theta}\right|^2}\cdot\left(1 - |\Gamma_L|^2\right). \quad (8)$$

Equation (8) is independent of the coupling factor. However, delivered power is a function of directivity of the coupler. Looking at (8), we conclude that, for higher directivity, $P_{\mathrm{out}}$ is less sensitive to phase variations at a fixed magnitude of the load reflection coefficient.

To illustrate how much impact directivity has on delivered power, we present two theoretical examples. In both cases, we choose load voltage standing wave ratio (VSWR) to be 6 : 1. This corresponds to having $|\Gamma_L|$ equal to 0.714. We set the available output power for the matched load to be 21 dBm. In one case, we chose directivity to be 15 dB and, in the other case, to be 0 dB. The resulting delivered power as a function of phase is shown in Fig. 15. The offset of 90° was added to make it easier for the reader to see the maximum and minimum of $P\mathrm{out}$.

We observe that 15-dB directivity can reduce the variation in the output power by over 13 dB. This is quite significant.

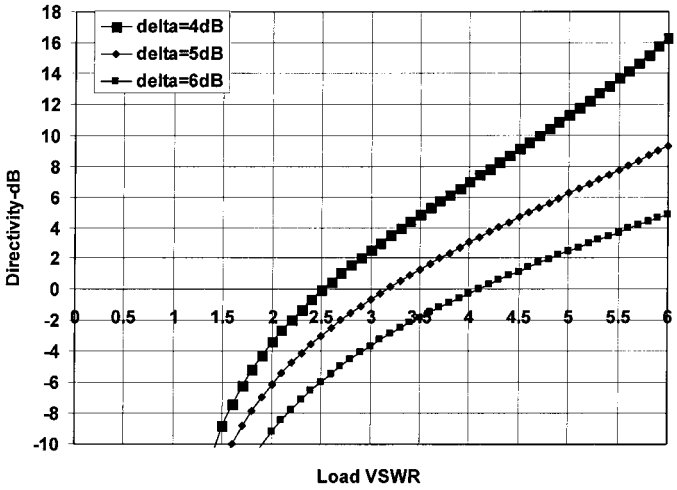


Fig. 16. Minimum directivity necessary to meet $+/-4$-dB power variation as a function of the load VSWR.

Now, let us go back to (8). The maximum and minimum output power is seen when $\theta$ is equal to 0° and $+/-180°$. For these two extreme cases, we can rewrite (8) as

$$P_{\max} = P_{\text{AVS0}} \frac{1-|\Gamma_L|^2}{\left(1-\frac{|\Gamma_L|}{D}\right)^2} \tag{9}$$

$$P_{\min} = P_{\text{AVS0}} \frac{1-|\Gamma_L|^2}{\left(1+\frac{|\Gamma_L|}{D}\right)^2}. \tag{10}$$

Equations (9) and (10) can be used to determine the minimum directivity required to ensure that the output power falls into the acceptable power range as defined by the standard. For example, if we assume that the nominal power transmitted by the PAM is set to $+21$ dBm, the maximum power variation that is allowed according to the GSM standard is $+/-4$ dBm. Therefore, we can write

$$P_{\text{AVS0}} - \delta \le P_{\text{out}} \le P_{\text{AVS0}} + \delta \tag{11}$$

where $P_{\text{AVS0}} = +21$ dBm and $\delta = 4$ dB. Substituting (9) and (10) into (11) and solving for $D$, we find

$$D \ge \frac{|\Gamma_L|}{\sqrt{\frac{1-|\Gamma_L|^2}{10^{-\frac{\delta}{10}}}-1}}. \tag{12}$$

The graph for the function in (12) is plotted in Fig. 16.

According to the graph in Fig. 16, if we assume that the maximum VSWR seen by the PAM is equal to $5:1$, then the minimum directivity needed to meet the specification is equal to 11.3 dB. If the directivity is less than that, the call may be dropped. As a reference, we also plotted (10) for $\delta = 5$ dB and $\delta = 6$ dB. These two values represent additional GSM standard tolerances for various power levels in the GSM900 and DCS1800 bands.

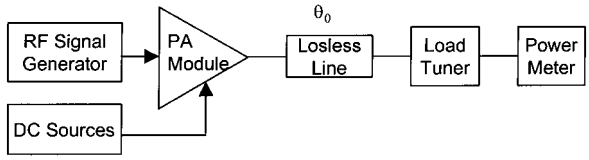


Fig. 17. Simplified block diagram of the load–pull setup.

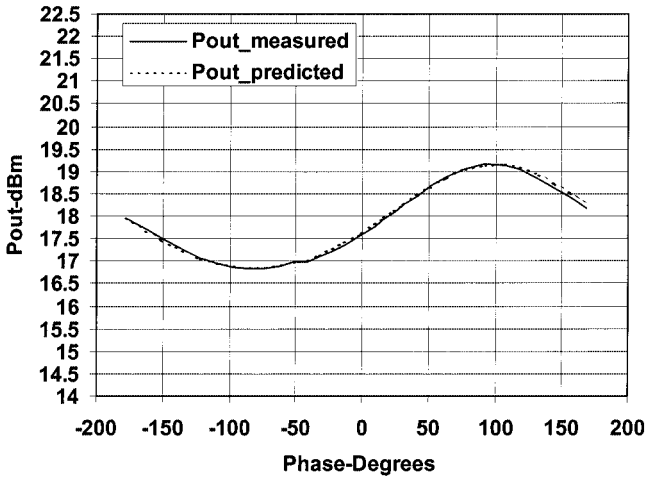


Fig. 18. Predicted versus measured results for our module with directional couplers; $\text{VSWR} = 6:1$.

## VI. Load–Pull Measurements

To verify the theoretical derivations presented in the previous section, we have measured several PAMs using a load–pull system. The simplified block diagram of the system used in our measurements is shown in Fig. 17.

$\theta_0$ in Fig. 17 is the phase associated with the lossless line that must be accounted for in the measurement data.

First, we characterized our module ADL5551. This module is the first to feature two integrated directional couplers. In these couplers, we have achieved $-30$-dB coupling and 14.3-dB directivity. The cost savings of having integrated couplers as opposed to the use of external ones is approximately \$0.17 per module.

We set the biasing to achieve 21-dBm available power and, thus, delivered power, in the matched load case. Higher values of power were not used to avoid saturation effects. At high values of VSWR, delivered power was a stronger function of phase. Equation (8) also predicts this. Most of the handset manufacturers are interested in module performance for VSWR up to $6:1$. Therefore, we chose this value to present our results. Fig. 18 shows measured and theoretical output power as a function of phase.

Here, the phase offset is approximately 79° to account for the length of the line on a test board. Also, we can see that high directivity of the couplers ensures a worst-case output power variation of $\pm 1.2$ dB. In addition, we observe that the theoretical predictions agree very well with the measured results. The errors fall within the tolerances of the load–pull system, as well as the slight imperfections in the power control circuitry.

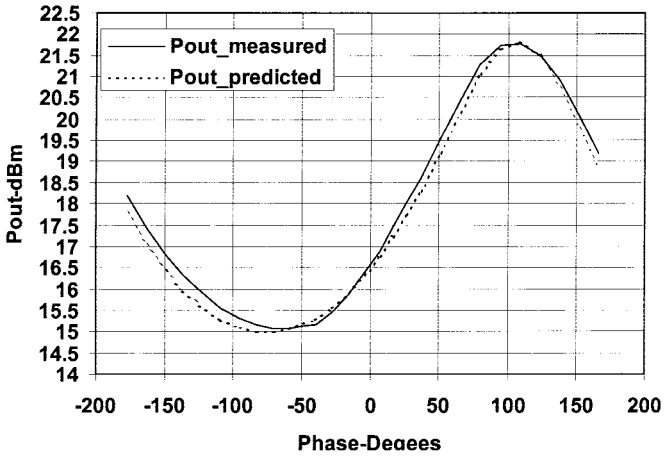


Fig. 19. Predicted versus measured results for module using open-loop controller without integrated couplers; $\mathrm{VSWR} = 6:1$.

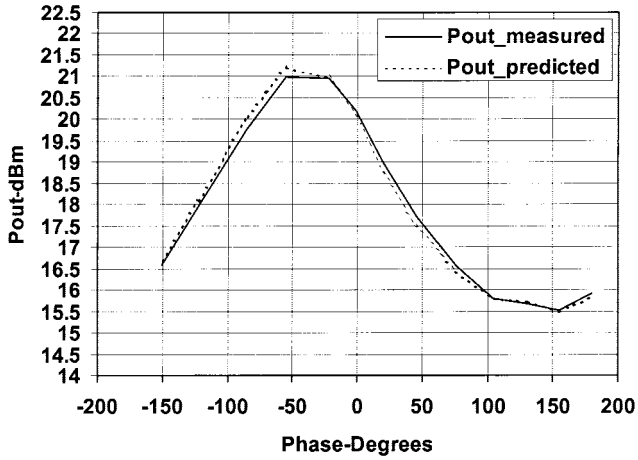


Fig. 20. Predicted versus measured results for module using current sensing; $\mathrm{VSWR} = 6:1$.

Next, in Figs. 19 and 20, we present results from the measurement of two major competitor commercial modules. One is using open loop control, and one is using current sensing with low directivity.

As we can see, competitor modules have output power variation that exceeds 6.5 dB in Fig. 19 and 5.5 dB in Fig. 20. For the measurement in Fig. 19, phase offset was approximately 164° and, for Fig. 20, it was approximately −137°. In Fig. 19, we also plotted $P_{\mathrm{out}}$ calculated using (8) with an estimated directivity of 5.5 dB. For Fig. 20, estimated directivity is 6.5 dB.

## VII. Conclusion

We have presented an advanced multichip quad-band PAM with unique linear-in-decibel output power dependency versus the set point voltage. The module incorporates a quad-band InGaP HBT PA and a state-of-the-art Si RF power detector and PA controller. The presented PAM offers 35- and 32.5-dBm output power at 900 and 1800 MHz, respectively. The novel output power control approach exhibits accuracy of +/−0.3 dB across a 50-dB power range. The PAM also features high efficiency, single positive power supply, single power control voltage, small size, and 50- to 50-Ω match from input to output terminals. The dimensions of the PAM are 10 × 10 × 1.5 mm. In addition, we showed that it is necessary to utilize high-directivity directional couplers in handset PAMs to achieve accurate power control. For a load VSWR of 6:1, we demonstrated that 14.3-dB directivity of the couplers reduces output power variation in our module by approximately 4 dB compared to other major competitor modules. We believe that our PAM provides OEMs a simple transmit solution, which will significantly reduce the overall cost and time to market for their products.

## Acknowledgment

The authors wish to thank Y. Zhao, R. Blanchard, E. Nash, and J. Bedrosian, all of Analog Devices Inc., Wilmington, MA, for their assistance and useful discussions.

## References

[1] "50 dB GSM PA controller," Analog Devices Inc., Wilmington, MA, AD8315 Datasheet, Rev. B. [Online]. Available: http://www.analog.com/UploadedFiles/Data_Sheets/848 367 596AD8315_b.pdf, 2003.

[2] S. Zhang *et al.*, "E-PHEMT, single supply, high efficient power amplifiers for GSM and DCS applications," in *IEEE MTT-S Int. Microwave Symp. Dig.*, vol. 2, May 20–25, 2001, pp. 927–930.

[3] "Quad band GSM/GPRS X-PA," Analog Devices Inc., Wilmington, MA, ADL5551/ADL5552 datasheet. [Online]. Available: http://www.analog.com/Analog_Root/productPage/productHome/0%2C2121%2CADL5551%2C00.html, 2003.

[4] S. Zhang *et al.*, "An advanced power amplifier module for quad-band wireless applications," in *Asia–Pacific Microwave Conf.*, Kyoto, Japan, Nov. 19–22, 2002.

[5] D. M. Pozar, *Microwave Engineering*. New York: Wiley, 1998.

**Shuyun Zhang** (M'02) was born in Jilin, China, in 1960. He received the B.S. degree in electronics engineering from the Harbin Institute of Technology, Harbin, China, in 1982, and the M.S. and Ph.D. degrees from Northeastern University, Boston, MA, in 1993 and 1996, respectively.

Prior to joining Analog Devices Inc., Wilmington, MA, in 2001, he designed numerous RF and microwave monolithic microwave integrated circuits (MMICs) for several different companies such as Hittite Microwave, M/A-COM, and Alpha Industries. He is currently a Senior Design Engineer with Analog Devices Inc., where he leads the development of PAMs for the wireless market. His research interests include modeling and design PA MMICs, switch/plexer, and fully integrated front-end modules for the handset market.

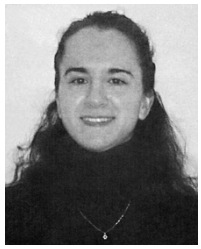

**Jelena Madić** (M'02) was born in Pančevo, Yugoslavia, in 1977. She received the Bachelor's and Master's degrees in electrical engineering and computer science from the Massachusetts Institute of Technology (MIT), Cambridge, in 2001 and 2002, respectively.

Upon graduation, she joined the Advanced Linear Products–RF Wireless (ALP–RFW) Group, Analog Devices Inc., Wilmington, MA, where she is currently an RF PA Design Engineer. Her interests include analog, RF, and mixed-signal design.

Ms. Madić is a member of Eta Kappa Nu and Sigma Xi.

**Pavel Bretchko** (S'98–M'01) was born in Tver, Russia, in 1973. He received the B.S. degree in microelectronics from the Moscow Engineering Physics Institute, Moscow, Russia, in 1995, and the M.S. and Ph.D. degrees from the Worcester Polytechnic Institute, Worcester, MA, in 1998 and 2001, respectively.

He is currently an RF PA Design Engineer with Analog Devices Inc., Wilmington, MA. His research interests include modeling and characterization of microwave devices, as well as the design and development of MMICs and modules for wireless communication applications.

**Julius Mokoro** received the A.S. Eng. degree in electrical engineering from Northern Essex Community College, Haverhill, MA, in 1992, the Sc. A.S. degree in electrical engineering from Middlesex Community College, Lowell, MA, in 1996, and the B.S. degree in electrical engineering from the University of Massachusetts Lowell, in 2002.

From 1995 to 2001, he was with Alpha Industries, Woburn MA. In 2001, he joined Analog Devices Inc., Wilmington, MA, where he is currently a Product Engineer with the RF Wireless (RFW) Group. His research interests include RF microwave PA design, advance PA test and measurement methodology, computer-aided design (CAD), and test software development.

**Raymond Shumovich** received the Bachelor of Science degree in electrical engineering from the Massachusetts Institute of Technology, Cambridge, in 1984, and the Master of Science degree (with a specialization in microwave engineering) from the University of Massachusetts at Amherst, in 1987.

He is currently a Senior Module Design Engineer with Analog Devices Inc., Wilmington, MA, where he assists in the design and production release of PAMs for various cell-phone applications. He was an RF MMIC and Module Designer for T/R modules for phased-array radar systems with the Advanced Device Center Raytheon, Andover, MA.

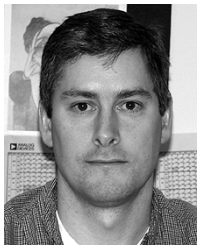

**Rob McMorrow** received the B.S.E.E. and M.S.E.E. degrees from Cornell University, Ithaca, NY, in 1988 and 1989, respectively. He also received business training at the Massachusetts Institute of Technology's (MIT) Sloan School of Management.

He is currently the Engineering Manager for RF PA products with Analog Devices Inc., Wilmington, MA, where he is responsible for overseeing the development of GaAs and SiGe PAMs for the cellular handset market. Prior to joining Analog Devices Inc., he held a similar position with Alpha Industries, where he helped to establish the company as a leader in GaAs ICs. He has also been with the Equipment Division Laboratories, Raytheon, where he designed GaAs MMICs. He has authored over ten papers and holds two patents.